

See discussions, stats, and author profiles for this publication at: <https://www.researchgate.net/publication/231677897>

Interaction Energy of Particles in Porous Media: New Deryaguin Type Approximation

ARTICLE in LANGMUIR · OCTOBER 1996

Impact Factor: 4.46 · DOI: 10.1021/la960074h

CITATIONS

8

READS

24

2 AUTHORS:



[Subir Bhattacharjee](#)

Water Planet Engineering

138 PUBLICATIONS **2,697** CITATIONS

SEE PROFILE



[Ashutosh Sharma IITK](#)

Indian Institute of Technology Kanpur

336 PUBLICATIONS **7,418** CITATIONS

SEE PROFILE

from the pore centerline.

$$d = r_w - r_p - r \quad (2)$$

For two quadratically curved surfaces, λ_m is related to the principal radii of curvature of the two surfaces at the points of closest approach: O_1 (radii R_{11} and R_{12}) and O_2 (radii R_{21} and R_{22}).^{10,11}

$$\lambda_m^2 = (R_{11}^{-1} + R_{21}^{-1})(R_{12}^{-1} + R_{22}^{-1}) + \sin^2 \phi (R_{11}^{-1} - R_{12}^{-1})(R_{21}^{-1} - R_{22}^{-1}) \quad (3)$$

where ϕ is the angle between the principal axes of the two surfaces. For the sphere-in-cylinder pore geometry, $\phi = 0$.^{10,11} For the particle-pore system of Figure 1, λ_m is easily obtained on the basis of the geometry (for the sphere, $R_{11} = R_{12} = r_p$; for the cylindrical pore, $R_{21} = -r_w$, $R_{22} = \infty$).

$$\lambda_m^2 = r_p^{-1}(r_p^{-1} - r_w^{-1}) \quad (4)$$

Equation 1 together with eqs 2 and 4 gives the particle-pore interaction energy when $\Delta G(L)$ for the system, *i.e.*, slab of particle material-liquid medium-slab of pore material, is known.

The apparent simplicity and universality of the Deryaguin approximation⁹⁻¹¹ leading to eq 1 are due to the following simplifications: (a) The intersurface distance is evaluated by approximating the sphere and the pore surfaces by parabolas passing through points O_1 and O_2 , respectively, in Figure 1b. In effect, the procedure replaces the actual bounded surfaces by unbounded surfaces P_1 and P_2 , which recede from each other indefinitely from around the points of the closest approach. The upper limit of the integral in eq 1 can thus be replaced by ∞ . (b) Ringlike differential surface area elements, with center around the axis O_1O_2 , are chosen on the surface P_1 (which represents the sphere in the vicinity of O_1) in order to evaluate the energy of interaction with the pore wall (surface P_2). (c) The interaction between the area element and the pore wall is approximately regarded as between two parallel surfaces; *i.e.* the local curvatures of the area element and the pore wall are neglected.

Because of the above approximations, the DA works best for the convex geometries, *e.g.*, sphere-sphere with radii large compared to the shortest distance. For such cases, the intersurface distance increases rapidly away from the points of closest approach, and contributions from the area elements far from O_1 are indeed insignificant. Further details and derivations of the DA and its limitations and its generalization for arbitrary curvatures (eq 3) may be found elsewhere.⁹⁻¹¹

Clearly, in the case of the particle-pore geometry (Figure 1), points away from O_1 and O_2 also contribute more significantly to the energy than is envisaged in the DA. In what follows, we relax approximations a and b discussed above. This is achieved by choosing the most general differential area element on the sphere surface and then summing up the interaction energy by the use of approximation c. Approximation c *cannot* be circumvented in *any* DA type approach where interactions between curved surfaces are predicted on the basis of the interaction energy of plane parallel half spaces, without resorting to a pairwise summation of intermolecular interactions.

In the new surface element integration (SEI) method developed here, the spherical particle is divided into a stack of cylindrical disks of thickness dz and radius, r_s , where $r_s^2 = r_p^2 - z^2$, and z is the axial distance of the disk from the sphere center (Figure 1). We now consider a

differential surface element (with surface area = $r_s dz d\theta$) on the curved surface of the cylindrical disk (Figure 1). The interaction energy of this differential element, dE_s with the surrounding pore wall is approximated as

$$dE_s \approx \Delta G(L) r_s d\theta dz \quad (5)$$

where L is now taken to be the distance between the surface of the differential element and the pore wall in the direction *normal* to the curved surface of the element. If we consider a cylindrical coordinate system (r, θ, z) as defined in Figure 1, the distance L is determined from the geometry as (Figure 1)

$$L = s_w - r_s = -r \cos \theta + [r_w^2 - r^2 \sin^2 \theta]^{1/2} - [r_p^2 - z^2]^{1/2} \quad (6)$$

The energy of interaction between the complete sphere surface and the pore wall is readily evaluated by integrating eq 5 to give

$$E_s = 4 \int_0^{r_p} \int_0^\pi [r_p^2 - z^2]^{1/2} \Delta G(L) dz d\theta \quad (7)$$

In view of expression 6, E_s from eq 7 has to be evaluated numerically when the form of ΔG is prescribed.

In contrast to the Deryaguin approximation, eq 7 does not assume the most significant contribution to the interaction energy comes only from the vicinity of points O_1 and O_2 , since contributions from all surface elements on the *actual* sphere surface are summed up in the SEI approach.

The accuracy of the Deryaguin approximation (eq 1) and the surface element integration method may be tested by considering those types of interactions for which the exact energy can be evaluated for the particle-pore geometry. The Lifshitz-van der Waals interactions provide the only possible test case, because, unlike the polar and electrostatic interactions,⁵ the LW interaction for the particle-pore geometry has been determined exactly^{3,4} on the basis of numerical summation of the pairwise intermolecular interactions in the microscopic approach of London and Hamaker.

The LW energy of interaction per unit area between two half spaces is given by $\Delta G(L) = -A/12\pi L^2$, where A is the effective Hamaker constant for the system (particle-liquid medium-pore wall). The interaction energy, E_p , from the DA can be easily evaluated analytically from eq 1. The comparison with the SEI is facilitated by a nondimensional representation of the interaction energy by defining

$$\rho = r/r_w, \quad \lambda = r_p/r_w, \quad \xi = z/r_w, \quad \text{and} \quad \eta = \rho/(1 - \lambda) \quad (8)$$

which convert eq 7 to a compact nondimensional form

$$E_s/A = -\frac{1}{3\pi} \int_0^\lambda \int_0^\pi [\lambda^2 - \xi^2]^{1/2} \delta^{-2} d\theta d\xi \quad (9)$$

where,

$$\delta = -\rho \cos \theta + [1 - \rho^2 \sin^2 \theta]^{1/2} - [\lambda^2 - \xi^2]^{1/2} \quad (10)$$

E_s/A is the nondimensional interaction energy, which is independent of the Hamaker constant, A . Simpson's rule with preset accuracy (automatic adjustment of grid spacing) was used for integration of eq 9. Figure 2 shows the comparison of the exact nondimensional interaction energy⁴ (solid lines) with the Deryaguin approximation

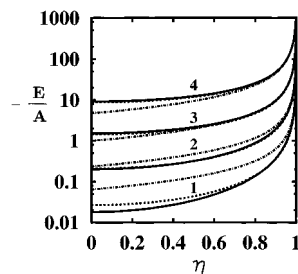


Figure 2. Comparison of the exact LW interaction energy (solid lines) with the Deryaguin approximation (nonuniformly broken lines) and the surface element integration method (uniformly broken lines). Curves 1–4 correspond respectively to $\lambda = 0.25, 0.5, 0.75$, and 0.9 . The results of the SEI coincide with the exact results for curves 2–4, i.e., for the $\lambda \geq 0.5$.

(nonuniformly broken lines) and the present approach (uniformly broken lines). Note that in Figure 2 negative of the nondimensional LW energy ($-E/A$) is plotted. The interpretation is as follows. The case of $A > 0$ ($E < 0$) corresponds to the LW attraction between the particle and the pore, whereas $A < 0$ ($E > 0$) denotes the LW repulsion.^{6,7} λ measures the size of the particle *relative* to the pore, and η is a nondimensional radial coordinate for the position of the particle. $\eta = 0$ corresponds to particles located at the pore centerline. The maximum possible values of λ and η (both less than 1) occur when the particle “contacts” the pore wall,⁴ i.e., $r = r_w - r_p - d_0$ or $r_p = r_w - d_0$, where d_0 (0.157 ± 0.009 nm) is a cutoff minimum equilibrium intersurface distance introduced by the short range Born repulsion.^{4,6,7} The cutoff distance also removes the (nonphysical) divergence of the LW interaction energy at “contact”.^{4,6,7} Thus, the maximum possible values of λ and η are $(0 \leq \lambda \leq \lambda_m; 0 \leq \eta \leq \eta_m)$ ⁴

$$\lambda_m = 1 - d_0/r_w, \quad \eta_m = (1 - \lambda - d_0/r_w)/(1 - \lambda) \quad (11)$$

While the above considerations of the LW cutoff are not exclusively related to our method (e.g., the flat plate interactions also diverge at $L = 0$), they are given here to illustrate the fact that η can be substantially smaller than 1 for many realistic combinations of the pore radius and λ , especially for tightly fitting particles ($\lambda \rightarrow \lambda_m$) in small pores (e.g., $\eta_m = 0.74$ for $\lambda = 0.8$ and $r_w = 3$ nm). In the hard-sphere approximation for the Born repulsion, the minimum in the interaction energy occurs at η_m for $A > 0$.

An inspection of Figure 2 reveals that the Deryaguin approximation works better for particles in immediate proximity to the wall ($\eta \rightarrow \eta_m$), but it seriously overestimates (at small λ) or underestimates (at large λ) the interaction energy of particles away from the wall. The surface element integration method is uniformly better, and its results virtually coincide with the exact results at all particle positions for moderate to large sized particles ($\lambda > 0.3$). To assess the accuracy of various approximations, we obtained the percent deviation defined as $[(\text{exact result} - \text{approximate result}) \times 100]/\text{exact result}$. The mean percent deviation of the DA in the range of η from

0 to 1 equals +20, +15, -70, and -330% for $\lambda = 0.8, 0.6, 0.4$, and 0.2 , respectively. The maximum percent deviations for the same values of λ are +40, +20, -100, and -500%, respectively. As is clear from the above and from inspection of Figure 2, errors in the DA increase both for high and low values of λ . This is because, for tightly fitting (high λ) particles, the entire sphere surface contributes to the energy, whereas, for low λ , the curvature effect becomes significant. Further, errors in the DA are not systematic in that the maximum deviation does not always occur at the pore centerline (e.g., curve 2 for $\lambda = 0.5$ in Figure 2). The mean and the maximum percent deviations (mean, maximum) for the SEI are (4, 5), (3, 4), (7, 12) and (40, 70) for $\lambda = 0.8, 0.6, 0.4$, and 0.2 , respectively. In contrast to the DA, the maximum deviation in the SEI occurs at the pore centerline, where the magnitude of the interaction energy is not as significant as that toward the pore wall. Even for particles much smaller than the pore size ($\lambda < 0.3$), the SEI method fares much better than the DA, but it still cannot be considered very accurate toward the pore centerline. This is however not a serious limitation, since whenever the SEI deviates from the exact results (e.g., $\eta < 0.6$ for $\lambda = 0.25$), the interaction energy is rather insignificant, i.e., $E < 0.1 A$, where A typically ranges from $1kT$ to $10kT$.

In conclusion, the SEI can be used for the more accurate determination of the interaction energy for particles in enclosed spaces whenever the energy is significant ($\geq kT$). While in the Deryaguin approximation, most of the interaction energy is contributed by regions very close to the points of shortest intersurface distance (O_1, O_2 in Figure 1), the SEI includes contributions from the entire sphere surface facing the enclosure. It is due to this reason that the DA but not the SEI becomes unsuitable for tightly fitting particles (high λ). As discussed earlier, the only (unavoidable) approximation in the SEI is the neglect of local curvatures in writing the interaction energy of the element in the form of eq 5. This approximation, which is also common to the DA, is responsible for the decreased accuracy of the SEI for relatively small (low λ , high curvature) particles located toward the pore centerline.

Finally, it is worth reiterating that as in the case for the Deryaguin approximation, the importance of the surface element integration approach lies not so much in evaluating the LW particle–pore interactions with greater ease but in the possibility of determining the other interaction energies (e.g. electrostatic, polar) for which exact results are either not available or not even theoretically possible presently (e.g., polar forces). The LW interaction energy merely provides a good test case, since the exact results are available. The SEI method can thus be used effectively to scale interaction energies for particles in enclosed spaces on the basis of the experimental knowledge of the interaction energy for the flat plate geometry. Evaluation of particle–pore forces other than the LW force by the SEI method and its application to transport in porous media and membrane separation will be published elsewhere.

LA960074H